

## Minimal path for transport in networks

W. R. Rossen\* and C. K. Mamun†

*Department of Petroleum Engineering, The University of Texas at Austin, Austin, Texas 78712*

(Received 21 September 1992; revised manuscript received 29 January 1993)

This report examines transport through networks in which transport across each bond in the network requires exceeding a microscopic threshold potential  $\Delta V_i^{\min}$ . In particular, we examine the macroscopic gradient  $\nabla V^{\min}$  at which transport begins, as a function of the distribution of microscopic thresholds  $\Delta V_i^{\min}$ . Applications of this “minimal path” or “breakdown” problem include electrical conduction through networks of diodes and the flow of Bingham plastics through porous media. Two simple models are examined, including a solution for  $\nabla V^{\min}$  for a Bethe- (or Cayley-) tree network. One simple model, based on taking the average of  $\Delta V_i^{\min}$  among the percolation-threshold fraction of low- $\Delta V_i^{\min}$  bonds, agrees remarkably well with both the Bethe-tree results and with the Monte Carlo studies for square and cubic networks. However, the Bethe-tree model shows that the minimal path samples the low end of this fraction most heavily. Doing so, it is aided by the existence of bonds with  $\Delta V_i^{\min}$  just above the value at the percolation threshold. Evidently the minimal path occasionally passes through these high- $\Delta V_i^{\min}$  bonds in order to access large clusters of low- $\Delta V_i^{\min}$  bonds.

### I. INTRODUCTION

Percolation theory is the study of transport through networks and inhomogeneous media.<sup>1</sup> In conventional bond percolation, a bond in a network is either open, with probability  $p$ , or closed, independent of the potential gradient  $\Delta V$  across the network. The percolation threshold,  $p_c$ , is the minimum value of  $p$  for which open bonds form a continuous path spanning an infinite network. In the flow of electrical current through random networks of diodes, or the flow of a Bingham plastic through random networks of tubes, however, a bond  $i$  is neither open nor closed intrinsically, but it is open if the potential drop across that bond  $\Delta V_i$  exceeds some randomly assigned threshold value  $\Delta V_i^{\min}$ . Transport across the network as a whole occurs if the macroscopic  $\nabla V$  exceeds some threshold  $\nabla V^{\min}$ . Related “breakdown” problems include conductivity and the onset of superconductivity in composites exhibiting a threshold voltage, fracturing of composite media, dielectric breakdown, elasticity of pilings with varying radii, ballistic particle deposition, the frontier of the Eden cluster, and directed polymers at zero temperature.<sup>2-8</sup>

Several authors have discussed the “minimal path” problem that defines the onset of transport in such a network and the magnitude of transport for  $\nabla V > \nabla V^{\min}$ . Roux, Hanson, and Guyon<sup>3</sup> and Roux and Herrmann<sup>9</sup> present Monte Carlo results for conductivity as a function of macroscopic  $\nabla V$  for transport in square networks exhibiting a distribution of  $\Delta V_i^{\min}$  values, with the network tilted at a 45° angle to the direction of flow. Sahimi<sup>8</sup> presents both an effective-medium solution and Monte Carlo results for square and cubic networks. All of these results were applied only to a distribution of  $\Delta V_i^{\min}$  that is uniform on the interval (0,1), however. In contrast, Stinchcombe, Duxbury, and Shukla<sup>10</sup> provide analytical and numerical solutions for the minimum  $\nabla V$

for transport on a Bethe (or Cayley) tree with  $\Delta V_i^{\min}$  taking only the extreme values on this interval, i.e., 0 and 1. Roux *et al.*<sup>7</sup> present an analytical solution for the onset of transport in a hierarchical diamond lattice. Yortsos<sup>11</sup> and de Gennes<sup>12</sup> consider the flow of Bingham plastics and foams in porous media. Adler and Brenner<sup>13</sup> discuss the flow of a Bingham plastic in a uniform fractal network. None of these studies have focused on how the distribution of  $\Delta V_i^{\min}$  values affects  $\nabla V^{\min}$ .

Related theoretical studies examine the shorting out of insulating bonds in an electrical network with  $p$  initially less than  $p_c$ ,<sup>14-16</sup> or the “burnout” of conducting bonds for  $p$  initially greater than  $p_c$ .<sup>14,17</sup>

There is an important difference between models in which breakdown occurs sequentially and irreversibly<sup>18</sup> and the minimal-path case examined here. The former can exhibit a size effect, in which, as the system size approaches infinity, the macroscopic  $\nabla V^{\min}$  reflects the minimum value of  $\Delta V_i^{\min}$ . In this case, the early local breakdown initiates a cascade effect that quickly disrupts the entire network. In our minimal path problem, however, no local transport (analogous to breakdown in the other models) occurs until a path for transport can form across the entire network. Therefore  $\nabla V^{\min}$  reflects a finite portion of the  $\Delta V_i^{\min}$  distribution.

Here we present two models for  $\nabla V^{\min}$ . The first is an extremely simple, approximate approach for any network for which the bond distribution  $\Delta V_i^{\min}$  and the percolation threshold are known. The second is a generalization of the solution of Stinchcombe, Duxbury, and Shukla<sup>10</sup> for a Bethe tree. Comparing these models illuminates the relation between the  $\Delta V_i^{\min}$  distribution, network structure, and  $\nabla V^{\min}$ , a topic unaddressed in earlier studies.

Our interest is motivated by the flow of foam through porous media,<sup>19-21</sup> which exhibits a threshold phenomenon similar to that of a Bingham plastic in networks of tubes. For Bingham plastics,<sup>22</sup> the potential  $V$

corresponds to pressure, and  $\Delta V_i^{\min}$ , the minimum pressure difference for flow between pores, depends on the yield stress of the fluid and on tube radius.

Foams of a fixed texture (bubble size) roughly approximate Bingham plastics in that the surface tension on individual films in the foams gives the foams an effective yield stress in porous media.<sup>23–27</sup> This yield stress traps up to 75–99 % of the foam in place in the pore space of rock even as injected foam travels through the remaining fraction of the pore space under massive applied pressure gradients.<sup>28,29</sup> The pore-size distribution of the rock evidently plays an important part in determining the fraction of the pore space through which foam flows. In bead packs, for instance, in which the pore-size distribution (and therefore the values of  $\Delta V_i^{\min}$ ) would be expected to be relatively uniform, a slight disturbance can completely alter the path along which foam flows.<sup>30</sup>

The Bingham model only roughly approximates flowing foams, in which the yield stress is focused at the discrete locations of the liquid films and not spread evenly across the fluid. However, the Bingham model exactly describes mobilization of a stationary foam in which liquid films occupy a fraction of the pore throats.<sup>31,33</sup> (Pore throats are the bonds or “tubes” in the pore network that link the nodes, called pore bodies.) In this case, the blocked bonds are assigned a finite threshold  $\Delta V_i^{\min}$  according to the pore-throat radius; for the unblocked bonds,  $\Delta V_i^{\min}=0$ . In this case the minimum pressure gradient to begin displacing these films defines the onset of “foam generation” in the porous medium.<sup>32</sup>

A brief preliminary report of this work appeared earlier.<sup>34</sup>

## II. SIMPLE PERCOLATION MODEL

The first model we present is a simple application of percolation concepts to the threshold for flow. In conventional percolation, a fraction of bonds equal to the percolation threshold  $p_c$  is sufficient to form a path for transport through the network.<sup>1</sup> If one assumes that the minimal path randomly samples the percolation-threshold fraction of bonds with the lowest  $\Delta V_i^{\min}$ , then  $\nabla V^{\min}$  is the average value of  $\Delta V_i^{\min}$  in this fraction:

$$\begin{aligned} \nabla V^{\min} &= \langle \Delta V_i^{\min} \rangle_p \\ &\equiv \int_0^{\Delta V_c} \nabla V_i^{\min} p^0(\Delta V_i^{\min}) d\Delta V_i^{\min} / p_c, \end{aligned} \quad (1)$$

where  $p^0(\Delta V_i^{\min})$  is the probability distribution for bond thresholds  $\Delta V_i^{\min}$  and  $\Delta V_c$  is given by

$$p_c = \int_0^{\Delta V_c} p^0(\Delta V_i^{\min}) d\Delta V_i^{\min}. \quad (2)$$

In (1) we have assumed for simplicity that each bond is one unit in length. We previously used (1) and (2) in estimating the minimum pressure gradient for flow of foams through pore networks.<sup>24</sup>

For the limiting case where  $\Delta V_i^{\min}$  takes only values of either 0 or 1, (1) and (2) indicate that  $\nabla V^{\min}=0$  if  $p \equiv p^0(0) \geq p_c$ , and  $\nabla V^{\min} = [(p_c - p)/p_c]$  if  $p < p_c$ . For the scaling region<sup>1</sup> of  $p$  near below  $p_c$ , this implies

$$\nabla V^{\min} \sim (p_c - p)^1. \quad (3)$$

This simple percolation model compares remarkably well to Sahimi’s<sup>8</sup> effective-medium approximation (EMA) and to Monte Carlo studies of two-dimensional (2D) and 3D square and simple cubic networks.<sup>3,4,9</sup> These studies assumed a bond-threshold distribution

$$\begin{aligned} p^0(\Delta V_i^{\min}) &= 1, \quad 0 \leq \Delta V_i^{\min} \leq 1 \\ &= 0, \quad \Delta V_i^{\min} > 1. \end{aligned} \quad (4)$$

For this distribution, Sahimi’s EMA predicts

$$\nabla V^{\min} = \frac{2}{Z} - \frac{2}{Z^2} = 0.375, \quad (5)$$

where  $Z$  is network coordination number,<sup>1</sup> while the simple-percolation model (1) predicts

$$\nabla V^{\min} = \int_0^{1/2} \Delta V_i^{\min} d\Delta V_i^{\min} / (1/2) = 0.25, \quad (6)$$

where we have applied the fact that  $p_c = 1/2$  both for square networks<sup>1</sup> and for EMA (Ref. 35) with  $Z = 4$ .

The Monte Carlo studies of Roux, Hanson, and Guyon<sup>3</sup> and Roux and Herrmann<sup>9</sup> found  $\nabla V^{\min} = 0.22$  to 0.23 for square networks tilted at a 45° angle to the direction of flow. For the tilted networks, these studies assumed the *projection* of a bond on the direction of flow was one unit in length. Sahimi’s<sup>8</sup> Monte Carlo study gives  $\nabla V^{\min} = 0.29$  for a square network aligned with the flow.

Table I summarizes these values along with similar results for the simple cubic network. The simple percolation model comes closer to the Monte Carlo results than does EMA. The simple percolation model cannot predict the rate of transport for  $\nabla V > \nabla V^{\min}$ , however.

Sahimi<sup>8</sup> points out that one expects  $\nabla V^{\min}$  to be lower for a tilted square network than one aligned with the flow. For the tilted network, two bonds at each node are

TABLE I. Predicted values of  $\nabla V^{\min}$  for networks with  $\Delta V_i^{\min}$  uniform on the interval (0,1).

Model	$\Delta V^{\min}$
Square network ( $Z = 4$ )	
Sahimi EMA <sup>a</sup>	0.375
Simple percolation model <sup>b</sup>	0.25
Monte Carlo studies	
Roux <i>et al.</i> <sup>c,d</sup>	0.227
Sahimi <sup>a</sup>	0.29
Roux and Herrmann (1987) <sup>e,e</sup>	0.22
Simple cubic network ( $Z = 6$ )	
Sahimi EMA <sup>a</sup>	0.278
Simple percolation model <sup>f</sup>	0.125
Sahimi Monte Carlo study <sup>a</sup>	~0.17

<sup>a</sup>Reference 8.

<sup>b</sup>Using  $p_c = 0.5$  (Ref. 1).

<sup>c</sup>Square network tilted at 45° angle.

<sup>d</sup>Reference 4.

<sup>e</sup>Reference 9.

<sup>f</sup>Using  $p_c = 0.2492$  (Ref. 1).

aligned equally with the flow, giving in effect two equal choices for the path at each node. In a square network aligned with the flow, however, only one bond points with the flow; therefore one must more frequently choose between a high- $\Delta V_i^{\min}$  bond aligned with the flow or a lower- $\Delta V_i^{\min}$  bond that does not point in the direction of flow. The issue of tortuosity—balancing minimal path length with minimizing the individual  $\Delta V_i^{\min}$  values in the path—was not addressed explicitly in any of these Monte Carlo studies. Presumably, the relatively uniform and compact  $\Delta V_i^{\min}$  distribution (4) assumed in these studies favors minimizing path length in most cases. For instance, Roux, Hanson, and Guyon<sup>3</sup> found virtually the same values of  $\nabla V^{\min}$  for directed and unrestricted percolation on their tilted square network. Clearly a short path, required in directed percolation, was close to the unrestricted minimal path.

The close agreement between the simple percolation model and the Monte Carlo studies may reflect two errors in the model that partially cancel each other: First, the simple percolation model assumes the path randomly samples the percolation-threshold fraction of low- $\Delta V_i^{\min}$  bonds (1), whereas the path may sample the low end of this fraction more heavily. This error tends to make the model overestimate  $\nabla V^{\min}$ . Second, the simple percolation model does not account for tortuosity, the need to occasionally increase path length in order to minimize overall  $\Delta V$ . This error tends to make the model underestimate  $\nabla V^{\min}$ .

The Bethe-tree model introduced in the next section corrects the first of these errors, but not the second.

### III. BETHE-TREE MODEL: DERIVATION OF $\nabla V^{\min}$

The simplest branched network is the Bethe (or Cayley) tree,<sup>1</sup> illustrated in Fig. 1. For the Bethe tree there are  $Z$  bonds joined at each node ( $Z=4$  in Fig. 1), but there is only one pathway between any two points. This

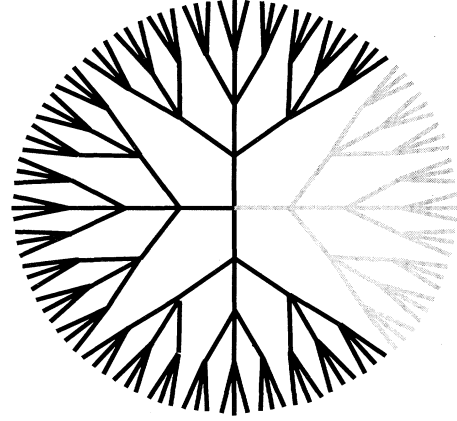


FIG. 1. Fragment of radius 4 from a Bethe tree of coordination number  $Z=4$ . One branch is highlighted.

property allows one to compute analytical formulas for the Bethe tree for properties that are approximated by EMA or must be estimated by Monte Carlo studies for two- and three-dimensional networks.<sup>1</sup> Here we define a single node as the center of a finite fragment of an infinite network and define the “radius” of the fragment as the number of bonds between the center and the edge (Fig. 1). We further define a “branch” of a fragment to be the set of all bonds forming paths between the center, through one of its  $Z$  connected bonds, to the edge. For a branch of radius  $n$ , the total potential difference required for transport  $\Delta V^{\min} \equiv n \nabla V^{\min}$  is the smallest value of  $\Sigma \Delta V_i^{\min}$  for any path from the center to the edge.

Our approach represents a generalization of that Stinchcombe, Duxbury, and Shukla<sup>10</sup> applied to the binary case where  $\Delta V_i^{\min}$  takes only values of 0 or 1. For that case, Stinchcombe, Duxbury, and Shukla showed that, for  $p \equiv p^0(0)$  just below  $p_c$ ,

$$\nabla V^{\min} \sim \frac{(p_c - p)/p_c}{1 + \ln(Z-2) - \ln \left[ \frac{p_c - p}{p_c} \right] + O \left[ \ln \ln \left[ \frac{p_c}{p_c - p} \right] \right]} \sim (p_c - p)^1 \quad (7)$$

as  $p$  approaches  $p_c$ . The scaling exponent of (7) thus matches that of the simple percolation model (3), but, as shown below, the simple percolation model substantially overestimates the value of  $\nabla V^{\min}$  for  $p$  near below  $p_c$ . Further from the percolation threshold, (7) suggests an apparent scaling exponent

$$\frac{d(\ln \nabla V^{\min})}{d[\ln(p_c - p)]} \sim 1 + \frac{1}{1 + \ln(Z-2) - \ln[(p_c - p)/p_c]} \quad (8)$$

Our approach, described below, is also similar to an approach Roux *et al.*<sup>7</sup> developed for the minimal path in a hierarchical diamond network.

One can derive a recursion formula for computing the probability distribution  $p_n$  for  $\Delta V^{\min(n)}$  for a Bethe-tree

branch of radius  $n$  from the probability distribution  $p_{n-1}$  for  $\Delta V^{\min(n-1)}$  for a Bethe-tree branch of radius  $(n-1)$  and  $p^0(\Delta V_i^{\min})$ :

$$p_n(\Delta V^{\min}) = \int_0^\infty \{ p^0(\Delta V_i^{\min} - x')(Z-1) p_{n-1}(x') \times [1 - \mathcal{P}_{n-1}(x')]^{Z-2} \} dx', \quad (9)$$

where  $p_n(\Delta V^{\min}) \equiv$  probability density function for  $[\Delta V^{\min(n)}]$  and

$$\mathcal{P}_n(x) \equiv \int_0^x p_n(x') dx'.$$

The derivation of (9) is illustrated in Fig. 2. It begins with  $p_{n-1}(\Delta V^{\min})$ , the probability distribution for  $\Delta V^{\min(n-1)}$  for a branch of length  $(n-1)$  from the

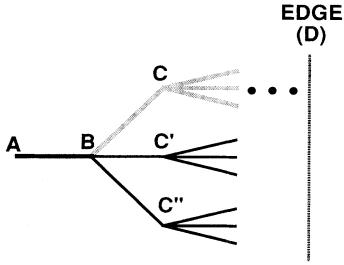


FIG. 2. Schematic derivation of Eq. (9).

center of a Bethe-tree fragment (e.g., the highlighted branch in Fig. 1).  $\Delta V^{\min}(n-1)$  is the minimum threshold for any path from point B through point C to the edge (D) in Fig. 2, while  $\Delta V^{\min}(n)$  is the minimum threshold for any path from point A through point B to the edge (D). Given  $p_{n-1}(\Delta V^{\min})$ , the probability of a given value of  $\Delta V^{\min}(n)$  is the joint probability, integrated over all values of  $x'$ , that (a) the first bond of the branch (i.e., from A to B has  $\Delta V_i^{\min} = (\Delta V^{\min} - x')$  and (b) the lowest-threshold path from there to the edge, from among the  $(Z-1)$  alternatives, has threshold  $x'$ . This second probability, in turn, is  $(Z-1)$  times the probability that (c) a given branch (for instance, BCD) has  $\Delta V^{\min}(n-1) = x'$  and (d) all of the  $(Z-2)$  alternatives have  $\Delta V^{\min} > x'$ . The factor  $(Z-1)$  accounts for the fact that the lowest-threshold path from point B to the edge could pass through any of the  $(Z-1)$  alternatives ( $C'$ ,  $C''$ , etc.).

The macroscopic minimum potential gradient for transport  $\nabla V^{\min}$  corresponds to the limit of  $(\Delta V^{\min}/n)$  as  $n \rightarrow \infty$ . (Again, for simplicity, we assume that bonds are one unit in length.) Evaluating the integral in (9) is numerically intensive and introduces small errors that could accumulate as  $n$  increases. Therefore, for computational purposes it is convenient to approximate the continuous variable  $\Delta V_i^{\min}$  with a rescaled discrete variable  $j$  that takes only integer values,  $0 \leq j < \infty$ . For this case the integral in (9) is replaced by a summation

$$p_n(j) = \sum_{i=0}^j p^0(j-i) \{ [1 - \mathcal{P}_{n-1}(i-1)]^{Z-1} - [1 - \mathcal{P}_{n-1}(i)]^{Z-1} \}, \quad (10)$$

where

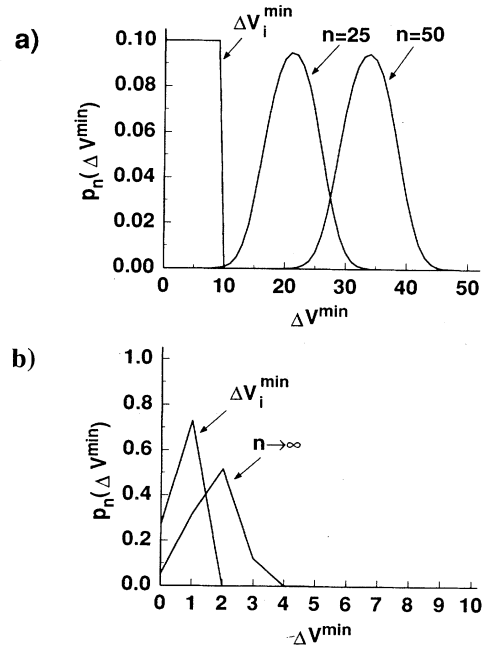
$$\mathcal{P}_n(i) \equiv \sum_{k=0}^i p_n(k)$$

and  $x$ ,  $\Delta V^{\min}$ , and  $\nabla V^{\min}$  correspond to  $i$ ,  $j$ , and  $j/n$ , respectively. The derivation of (10) is as follows: The probability that the minimum threshold is  $j$  for a path of length  $n$  is the product of the probabilities that the first bond has threshold  $(j-i)$  and that the rest of the path has threshold  $i$ . This latter probability is the difference between the probabilities that all  $(Z-1)$  paths from there to the edge have threshold greater than  $(i-1)$  and that all  $(Z-1)$  paths have threshold greater than  $i$ . The different form of (10) compared to (9) reflects the finite probability that two branches have the same value of

$\Delta V^{\min}(n-1)$ , an event of zero probability if  $\Delta V_i^{\min}$  is a continuous variable. There is no accumulating error in recursively evaluating the summation in (10) comparable to that introduced in numerically evaluating the integral in (9). Therefore we have used (10) in the results presented here.

The behavior we observe with (10) mimics that observed by Stinchcombe, Duxbury, and Shukla<sup>10</sup> for relatively small values of  $n$  and a binary  $\Delta V^{\min}$  distribution. Figure 3 shows the two types of behavior we have observed. Both cases were computed for discrete  $\Delta V_i^{\min}$  and  $\Delta V^{\min}$ , and in both cases  $Z=5$ . In Fig. 3(a),  $\Delta V_i^{\min}$  takes integer values between 0 and 9, each with probability 0.1. In Fig. 3(b),  $\Delta V_i^{\min}$  takes values 0 (with probability 0.26) or 1 (with probability 0.74). In both cases, for convenience we plot the discrete variable  $\Delta V^{\min}$  as though continuous.

As  $n \rightarrow \infty$ , one of two events occurs. Either  $p_n(\Delta V^{\min})$  attains a constant shape and moves towards increasing  $\Delta V^{\min}$  at a constant rate with increasing  $n$ , or it attains a constant shape anchored to a finite probability of a zero threshold for the network as a whole. The constant shape of  $p_n(\Delta V^{\min})$  means that the variance of the  $p_n(\Delta V^{\min})$  approaches a constant value as  $n \rightarrow \infty$ . This in turn implies that the variance of the probability distribution for  $\nabla V^{\min} \equiv (\Delta V^{\min}/n)$  approaches zero as  $n \rightarrow \infty$ ; in other words, all realizations of  $\nabla V^{\min}$  approach the average value as  $n \rightarrow \infty$ . This further means that our algorithms (9) and (10), based on the threshold for flow of one branch of a Bethe tree as shown in Fig. 2, applies to the entire Bethe tree as well.  $\nabla V^{\min} = \Delta V^{\min}/n$  approaches zero for large  $n$ , as in Fig. 3(b), if  $p^0(0) \geq p_c$  — i.e., if there is a sufficiently large fraction of bonds with

FIG. 3. Two types of behavior of Bethe-tree model with increasing  $n$ .

zero threshold to form a zero-threshold path across an infinite network. In any case, the constant or zero value of  $(\Delta V^{\min}/n)$  attained as  $n \rightarrow \infty$  is the asymptotic value  $\nabla V^{\min}$  for large networks.

The unchanging shape of  $p_n(\Delta V^{\min})$  as  $n$  increases suggests an analogy between the recursion formulas (9) and (10) and "self-sharpening" partial differential equations, like the Buckley-Leverett equation for flow through porous media,<sup>36,37</sup> that give rise to propagating fronts of

permanent form.<sup>38</sup> Stinchcombe, Duxbury, and Shukla<sup>10</sup> assumed this sort of behavior in deriving their scaling result (8) for  $p$  near below  $p_c$ . The development of such an unchanging front, with constant velocity  $\nabla V^{\min}$ , as  $n$  increases, implies that as  $n \rightarrow \infty$

$$p_n(\Delta V^{\min}) = p_{n-1}(\Delta V^{\min} - \nabla V^{\min}) . \quad (11)$$

Substituting  $p_{n-1}(\Delta V^{\min} - \nabla V^{\min})$  for  $p_n(\Delta V^{\min})$  in (9) gives

$$0 = -p_{n-1}(\Delta V^{\min} - \nabla V^{\min}) + \int_0^\infty \{p^0(\Delta V^{\min} - x')(Z-1)p_{n-1}(x')[1 - \mathcal{P}_{n-1}(x')]^{Z-2}\} dx' (n \rightarrow \infty) . \quad (12)$$

If one defines

$$x \equiv \Delta V^{\min} - \nabla V^{\min} n + C , \quad (13)$$

with  $C$  an arbitrary constant, and lets

$$p_\infty(x) \equiv \lim_{n \rightarrow \infty} p_{n-1}(x + \nabla V^{\min} n + C) \quad (n \rightarrow \infty) , \quad (14)$$

then (12) implies

$$0 = -p_\infty(x - \nabla V^{\min}) + \int_0^\infty \{p^0(x - x')(Z-1)p_\infty(x')[1 - \mathcal{P}_\infty(x')]^{Z-2}\} dx' . \quad (15)$$

Here  $\mathcal{P}_\infty$  is the integral of  $p_\infty$ , as  $\mathcal{P}_n$  is the integral of  $p_n$  in (9).

The unknown scalar  $\nabla V^{\min}$  and function  $\mathcal{P}_\infty(x)$  can be determined from (15) using, for instance, finite-difference or finite-element integration schemes; one needs initial guesses for both  $\nabla V^{\min}$  and  $\mathcal{P}_\infty(x)$ , and one must fix one value of the function  $\mathcal{P}_\infty(x)$  [equivalent to setting  $C$  in (13)] arbitrarily.

Roux *et al.*<sup>7</sup> derive roughly similar approach for the hierarchical diamond lattice. There, each recursion doubles the length of the network. They derive a recursive formula for  $\nabla V^{\min}$  and show that a single integral equation describes the asymptotic shape of a rescaled  $p_\infty(x)$  for a wide class of functions  $p^0(\Delta V_i^{\min})$ .

A somewhat more complex formula than (15) applies when  $\nabla V_i^{\min}$  takes only integer values as in (10). The complication arises because  $\nabla V^{\min}$  may be a fraction, while  $p^0(j)$ ,  $p_n(j)$ , and  $\mathcal{P}_n(j)$  are defined only at integer values of  $j$ . Therefore, if the integer portion of  $\nabla V^{\min}$  is  $k$  and the fractional part is  $f$ , with  $0 \leq f \leq 1$ , we approximate  $p_{n-1}(j - \nabla V^{\min})$  by a linear interpolation between the values at the nearest integer coordinates [i.e., at  $(j-k)$  and at  $(j-k-1)$ ]:

$$p_{n-1}(j - \nabla V^{\min}) \equiv (1-f)p_{n-1}(j-k) + fp_{n-1}(j-k-1) . \quad (16)$$

Then substituting  $p_{n-1}(j - \nabla V^{\min})$  for  $p_n(j)$ , and  $p_\infty(j)$  for  $p_{n-1}(j)$ , into (10) gives an analog to (15)

$$0 = (1-f)p_\infty(j-k) + fp_\infty(j-k-1) - \sum_{i=0}^j p^0(j-i) \{ [1 - \mathcal{P}_\infty(i-1)]^{Z-1} - [1 - \mathcal{P}_\infty(i)]^{Z-1} \} , \quad (17)$$

where

$$\mathcal{P}_\infty(i) \equiv \sum_{k=0}^i p_\infty(k) .$$

If  $j$  varies from 0 to some large integer  $N$ , then (17) represents a set of  $(N+1)$  nonlinear algebraic equations to be solved for unknown scalar  $\nabla V^{\min} \equiv k + f$  and vector  $\mathcal{P}_\infty(j)$ . One element of the vector  $\mathcal{P}_\infty(j)$  (preferably near the middle of the vector) may be set arbitrarily. Newton-Raphson or some similar scheme may be used to solve this equation set given an initial guess of  $\nabla V^{\min}$  and  $\mathcal{P}_\infty(j)$ . One should select a value of  $N$  large enough that  $\mathcal{P}_\infty(j)$  approaches zero for small values of  $j$  and 1 for large values of  $j$ , in order to minimize numerical artifacts introduced by excluding the infinite range of  $j$  possible in principle as  $n \rightarrow \infty$ .

Equation (17) provides an independent check on the numerical accuracy of the solution to the recursion Eq. (10). Questions of numerical accuracy are addressed in the following section.

#### IV. NUMERICAL ACCURACY OF SOLUTIONS FOR BETHE TREE

The first source of numerical error is the possible accumulation of roundoff errors in recursively evaluating (10) for large  $n$ . Such a roundoff error would become evident through probability functions that no longer sum to 1 as  $n$  increases. We found, however, that the calculations were "stable," i.e., the sum over  $j$  of  $p_n(j)$  equaled 1 to within approximately the machine roundoff error for all calculations regardless of the magnitude of  $n$ . In other words, roundoff errors in solving (10) did not accumulate and grow as  $n$  increased.

We performed these calculations on both Vax 6000 and

CDC 170/750 computers. For these machines, the inherent roundoff error  $\epsilon$  was roughly  $0.7 \times 10^{-17}$ . In other words, the smallest positive number the computer could subtract from 1 and get a number less than 1 was  $\epsilon$ .

There was a significant roundoff problem that was subsequently eliminated. If  $p_c > p^0(0) > p_c/2$ , then the function  $p_n(j)$  would remain anchored at zero as in Fig. 3(b) as  $n \rightarrow \infty$ ; that is,  $p_n(0)$  remained finite and positive as  $n \rightarrow \infty$ . This behavior was expected only if  $p^0(0) \geq p_c$ . To see the source of the artifact, consider a case where, after some recursions,  $p_n(0) = \epsilon$ . From (10),

$$\begin{aligned} p_{n+1}(0) &= p^0(0) \{1 - [1 - \epsilon(Z - 1)]\} \\ &\sim p^0(0)(Z - 1)\epsilon = \epsilon p^0(0)/p_c, \end{aligned} \quad (18)$$

since, for the Bethe tree,  $p_c = 1/(Z - 1)$ .<sup>1</sup> If  $p^0(0)/p_c \geq 0.5$ ,  $p_{n+1}(0)$  decreases by less than half from  $p_n(0)$ , and the machine rounded  $p_{n+1}(0)$  up to its smallest positive number (i.e., back to  $\epsilon$ ); if  $p^0(0)/p_c < 0.5$ , the machine rounded  $p_{n+1}(0)$  down to zero. One could avoid this false rounding of  $p_{n+1}(0)$  up to a constant positive number by requiring that any  $p_n(j)$  be reduced to zero if  $p_n(j)$  is less than some threshold  $\epsilon^* > \epsilon$  and if  $p_n(j - 1)$  is zero. This eliminated the artifact. Subsequent solutions did not change as the value of  $\epsilon^*$  was varied by several orders of magnitude above the machine roundoff error  $\epsilon$ .

To determine  $\nabla V^{\min}$  from the vector  $p_n(j)$ , we first determined the mean  $\mu_n$  of the distribution  $p_n(j)$  for each value of  $n$ , and then determined  $d\mu_n/dn$  from a fifth-order polynomial fit to  $\mu_n$  using consecutive values of  $n$ . For most cases a virtually constant  $d\mu_n/dn$  was obtained within a few tens of recursions.

For discrete distributions  $\Delta V_i^{\min}$  and  $\Delta V^{\min}$ , however, the function  $p_n(j)$  cannot form a strictly unchanging front and move with a constant velocity as  $n$  increases; the shape and velocity are distorted by the underlying discrete coordinate grid of integer values of  $j$ . This means that instead of taking an absolutely constant value,  $\nabla V^{\min}$  fluctuates about a constant value as  $n \rightarrow \infty$ , with the period of the oscillation approximating the number of recursions required to advance the front one integer grid point. Stinchcombe, Duxbury, and Shukla<sup>10</sup> did not observe these oscillations, possibly because their numerical results were limited to relatively large values of  $(p_c - p)$  and small values of  $n$ . To estimate the underlying constant velocity of the front, we plotted  $d\mu_n/dn$  values as a function of  $1/n$  and determined the mean and width of the oscillations. For most cases, the stable oscillations set in at practicable values of  $n$  and the oscillations were small. However, for  $p^0(0)$  very near  $p_c$ , the period of the oscillations became so large (because  $\nabla V^{\min}$  was so small) that tens of thousands of recursions were required to traverse one period in the oscillation. Typically  $d\mu_n/dn = \nabla V^{\min}$  decreased as  $1/n$  decreased, then began to fluctuate about a constant value as  $1/n \rightarrow 0$ . An example is shown at the top of Fig. 4. Here  $Z = 3$  and bonds have either  $\nabla V_i^{\min} = 0$ , with probability  $p^0(0) \equiv p$ , or  $\Delta V_i^{\min} = 1$ . For  $Z = 3$  the percolation threshold on a Bethe tree is 0.5. Therefore, for  $p = 0.495 < p_c$ ,  $d\mu_n/dn$  oscillates about a positive value of  $\nabla V^{\min}$  as  $n \rightarrow \infty$ . For

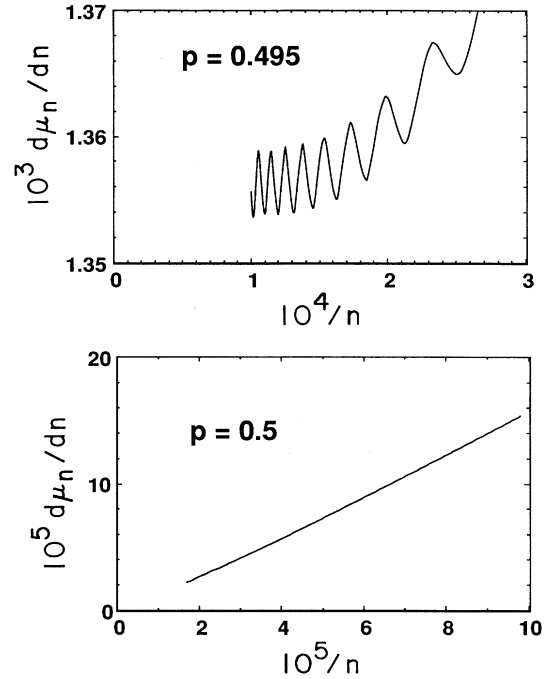


FIG. 4. Trends of  $d\mu_n/dn$  with  $n$  for binary bond-threshold distribution and  $Z = 3$ .

$p^0(0) > p_c$  (not shown),  $d\mu_n/dn$  rapidly approaches zero at finite  $n$ . As shown at the bottom of Fig. 4, for  $p^0(0) = 0.5 = p_c$ ,  $d\mu_n/dn$  approaches zero asymptotically as  $1/n \rightarrow 0$ . As noted, for  $p^0(0) < p_c$ ,  $d\mu_n/dn$  oscillates about a fixed value as  $n \rightarrow \infty$ ; we report here only cases where the oscillation had stabilized within the number of recursions tested.

Fortunately, given the uncertainty in  $\nabla V^{\min}$  determined recursively using (10) due to the oscillations in  $d\mu_n/dn$ , (17) gives an independent estimate of  $\nabla V^{\min}$ . Equation (17) also reflects the discrete grid in  $j$  imposed on the problem [cf. (16)]. In this case, distortions to behavior imposed by (16) should manifest themselves in differences between cases run with different values for the one element of  $\mathcal{P}_\infty(j)$  that is set arbitrarily. These differences reflect different frontal positions of  $\mathcal{P}_\infty$  on the underlying coordinate grid. We found, however, excellent agreement both between the solutions using (10) and (17) and using (17) with different values for this element.

The oscillations of  $d\mu_n/dn$  as  $n$  approaches infinity does not appear to violate the assumption that  $\nabla V^{\min}$  approaches a "thermodynamic limit," as used by Stinchcombe, Duxbury, and Shukla<sup>10</sup> to derive (7). Though  $d\mu_n/dn$ , the derivative of  $\Delta V^{\min}(n)$ , oscillates, the magnitude of these fluctuations in  $\nabla V^{\min} = \Delta V^{\min}/n$  approaches zero as  $n \rightarrow \infty$ .

Surprisingly, however, our numerical results do not fit (8) for the case of binary  $\Delta V_i^{\min}$ . Table II shows apparent exponents fitted to log-log plots of  $\nabla V^{\min}$  and  $(p_c - p)$  such as Fig. 5 for several values of  $Z$ . The exponents are all a little greater than 1, in agreement with (8). Howev-

er, (8) suggests that the apparent exponent should depend on  $Z$ , whereas our results for all values of  $Z$  had nearly the same apparent exponent. Figure 6 shows the residuals from the fit of the apparent scaling exponent for  $Z=9$ , a typical case. The various data shown for each value of  $(p_c - p)$  include the results using the recursion formula (10) and using (17) with several different values of the arbitrary datum in the vector  $\mathcal{P}_\infty(j)$ . There is a systematic trend to the residuals, with a distinct non-linearity for  $(p_c - p)$  less than about  $10^{-3}$ , in agreement with (8). However, the fit to the linear portion for

$(p_c - p) \geq 10^{-3}$  gives virtually the same exponent, 1.1212, as the fit over the entire interval (Table II). Equation (8) indicates that the apparent exponent should vary more strongly with  $(p_c - p)$ . We do not know the cause of these apparent discrepancies.

## V. RESULTS

Figure 7 compares the two models for  $\nabla V^{\min}$  presented here for a log-normal distribution of  $\Delta V_i^{\min}$ :

$$p^0(\Delta V_i^{\min}) = (2\pi\sigma^{*2})^{-1/2} \exp\left[-\frac{(\ln\Delta V_i^{\min} - \ln\Delta V_i^{\min*})^2}{2\sigma^{*2}}\right] \frac{1}{\Delta V_i^{\min}}, \quad (19)$$

where  $\sigma^*$  and  $\ln\Delta V_i^{\min*}$  are model parameters. This log-normal distribution for  $\Delta V_i^{\min}$  corresponds to a log-normal distribution of pore-throat sizes, which control the minimum pressure gradient for flow of a Bingham plastic in a porous medium. In the case shown in Fig. 7, with  $\sigma^* = 1.15$ , 95% of the distribution lies within a factor of 10 of the logarithmic mean value  $\Delta V_i^{\min*} = 15$ ; the arithmetic mean value is 24.5. The two models compared in Fig. 7 are a Bethe tree with  $Z=5$  and the simple percolation model with  $p_c$  assumed to be 0.25 as for the Bethe tree. For consistency we used a discrete approximation to the continuous  $\Delta V_i^{\min}$  distribution for computations involving both models. This distribution is illustrated by the discrete points in Fig. 7. In principle, this distribution should extend to  $\Delta V_i^{\min} \rightarrow \infty$ ; in practice we truncated the distribution at a single large value of

$\Delta V_i^{\min}$ , i.e., 100, and lumped the cumulative remainder of the tail of the distribution at this value. This truncation had no effect on the results, because the onset of transport is dominated by small values of  $\Delta V_i^{\min}$ .

We cannot compare published Monte Carlo results<sup>3,4,8,9</sup> or Sahimi's<sup>8</sup> EMA directly to these predictions because all these studies focused on a uniform  $\Delta V_i^{\min}$  distribution.

The computed value of  $\nabla V^{\min}$  for the Bethe tree is about 25% lower than the simple-percolation-model estimate. The solution for the Bethe-tree model differs from the simple percolation model in two ways: (1) The simple percolation model assumes that the path for the onset of flow samples randomly from the percolation-threshold fraction of bonds with lowest  $\Delta V_i^{\min}$ , whereas the path may in fact sample more heavily from the lowest- $\Delta V_i^{\min}$  values. (2) The Bethe-tree solution allows the path for the onset of flow to sample an occasional bond with a large  $\Delta V_i^{\min}$  if it can thereby access a large cluster of low- $\Delta V_i^{\min}$  bonds and reduce the overall  $\nabla V^{\min}$ . The two differences are related, in that freedom to pass through an occasional large- $\Delta V_i^{\min}$  bond may allow access to a large cluster of small- $\Delta V_i^{\min}$  bonds.

To distinguish between these mechanisms we determined  $\nabla V^{\min}$  for several bond-threshold distributions that differ in (a) the skewness of the low end of the  $\Delta V_i^{\min}$  distribution and (b) the existence of values of  $\Delta V_i^{\min}$  just above the percolation-threshold value  $\Delta V_c$  (2). All of the

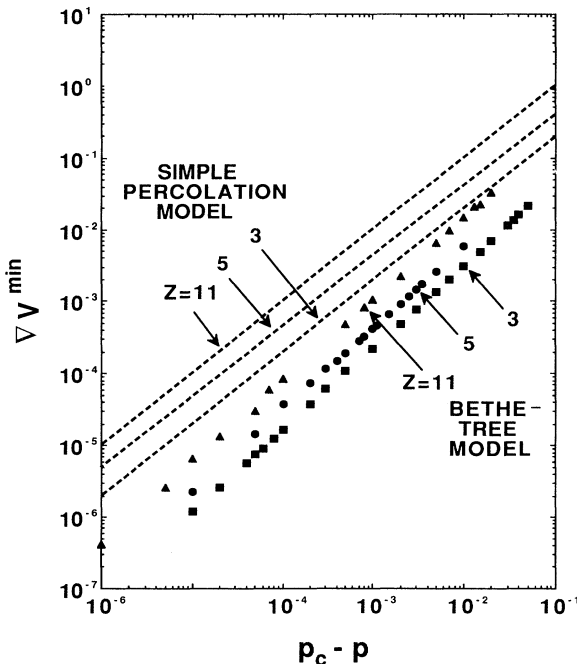


FIG. 5. Predicted  $\nabla V^{\min}$  for binary  $\Delta V_i^{\min}$  distribution.

TABLE II. Apparent exponent for scaling of  $\nabla V^{\min}$  with  $(p_c - p)$  for binary distribution of  $\Delta V_i^{\min}$ .

$Z$	Apparent exponent	Range of $(p_c - p)$
3	1.1203	$1 \times 10^{-2} - 2 \times 10^{-4}$
5	1.1219	$5 \times 10^{-3} - 2 \times 10^{-4}$
6	1.125	$8 \times 10^{-3} - 5 \times 10^{-5}$
9	1.1222	$8 \times 10^{-3} - 5 \times 10^{-5}$
11	1.1215	$1.5 \times 10^{-2} - 5 \times 10^{-5}$
17	1.1214	$1.25 \times 10^{-2} - 5 \times 10^{-5}$
21	1.1215	$5 \times 10^{-3} - 5 \times 10^{-5}$

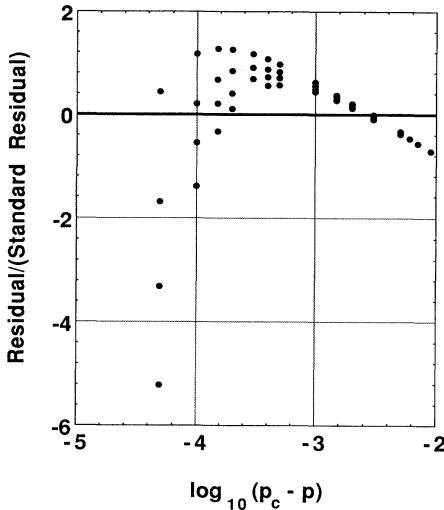


FIG. 6. Residuals from fit to scaling equation for  $Z=9$ .

distributions we tested comprise only integer values of  $\Delta V_i^{\min}$  and  $\nabla V^{\min}$ . The six distributions we tested for  $Z=5$  are illustrated in Fig. 8; we tested a similar set of six cases for  $Z=11$ . For each value of  $Z$ , we tested three types of  $\Delta V_i^{\min}$  distribution: a uniform distribution, and two log-normal distributions (19) with, respectively,  $\sigma^*=1$  and  $\sigma^*=0.25$ . In all cases, the values of  $\Delta V_i^{\min}$  from 1 to 10 comprise exactly the percolation-threshold fraction of the entire distribution (10% for  $Z=11$  and 25% for  $Z=5$ ), and the portion of the distribution with  $\Delta V_i^{\min} > 50$  is lumped into the fraction at  $\Delta V_i^{\min}=50$ . For each of the three types of  $\Delta V_i^{\min}$  distribution, we tested also a similar distribution truncated just above the

percolation threshold, with the remaining fraction lumped at  $\Delta V_i^{\min}=50$ .

The simple percolation model predicts that  $\nabla V^{\min} = \langle \Delta V_i^{\min} \rangle_p$ , the average of  $\Delta V_i^{\min}$  for  $\Delta V_i^{\min} \leq \Delta V_c$  [Eqs. (1) and (2)]. Therefore the simple-percolation estimate of  $\nabla V^{\min}$  is unaffected by truncating the  $\Delta V_i^{\min}$  distribution above  $\Delta V_c$ . For the uniform  $\Delta V_i^{\min}$  distributions, regardless of the value of  $Z$ , the simple-percolation estimate of  $\nabla V^{\min}$  is 5.5, because  $\langle \Delta V_i^{\min} \rangle_p$  is the average of the integers between 1 and 10. For the other distributions the simple-percolation estimate is higher, because the  $\Delta V_i^{\min}$  distributions are grouped closer to the percolation-threshold cutoff between  $\Delta V_i^{\min}=10$  and 11 (Fig. 8).

Values of  $\nabla V^{\min}$  computed for the Bethe tree with these  $\Delta V_i^{\min}$  distributions are summarized in Table III and Fig. 9. These results show that  $\nabla V^{\min}$  reflects (1)  $\langle \Delta V_i^{\min} \rangle_p$ , the average value of  $\Delta V_i^{\min}$  for  $\Delta V_i^{\min} \leq \Delta V_c$  [Eqs. (1) and (2)], (2) the existence of a tail of low- $\Delta V_i^{\min}$  values well below  $\langle \Delta V_i^{\min} \rangle_p$ , and (3) the existence of  $\Delta V_i^{\min}$  values just above  $\Delta V_c$ . The simple-percolation model reflects only the first of these trends.

The Bethe-tree model also follows the first trend:  $\nabla V^{\min}$  is indeed larger for the cases where  $\langle \Delta V_i^{\min} \rangle_p$  is larger. There are subtler trends, however, that are made clear by rescaling the values of  $\nabla V^{\min}$ . Since the total

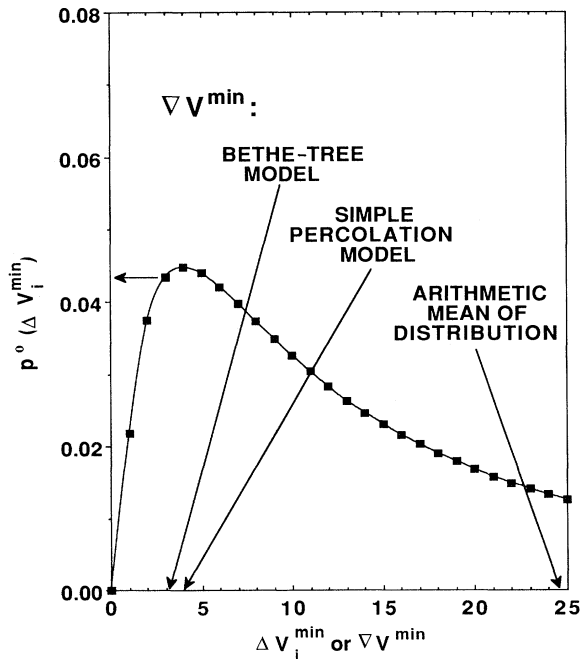


FIG. 7. Network models for  $\nabla V^{\min}$ .

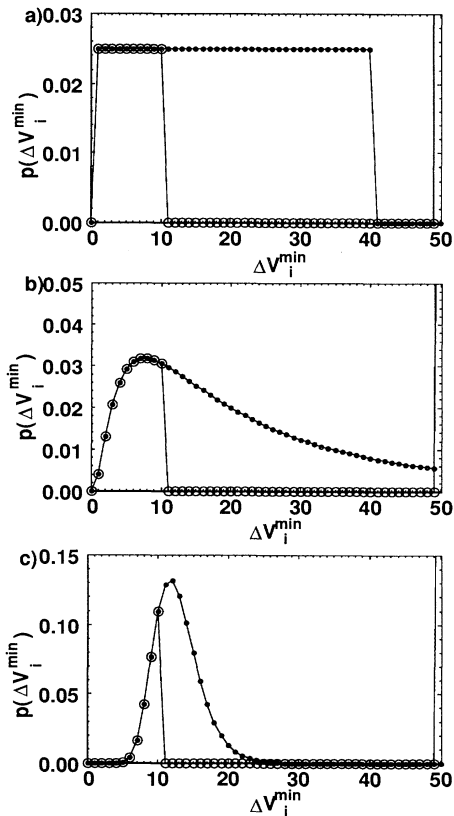


FIG. 8. Sample bond-threshold distribution functions for  $Z=5$ . (a) Uniform; (b) log-normal,  $\sigma^*=1$ ; (c) log-normal,  $\sigma^*=0.25$ . Open symbols: truncated distribution.



TABLE III. Effect of bond-threshold distribution on  $\nabla V^{\min}$  for Bethe-tree network. In all cases, percolation-threshold fraction includes integer elements in interval  $1 \leq \Delta V_i^{\min} \leq 10$ . (For  $Z=5$ , percolation threshold is 0.25; for  $Z=11$ , 0.10.) The portion of distribution with  $\Delta V_i^{\min} > 50$  is lumped into fraction with  $\Delta V_i^{\min} = 50$ .

Case description	$\Delta V^{\min}$		Rescaled Bethe tree
	Simple percolation model, $\langle \Delta V_i^{\min} \rangle_p$	Bethe tree	
<b>Z = 5</b>			
Uniform	5.500	4.211	4.211
Same, truncated	5.500	4.929	4.929
Log-normal, $\sigma^* = 1$	6.385	5.230	4.096
Same, truncated	6.385	5.928	4.945
Log-normal, $\sigma^* = 0.25$	9.084	8.420	3.157
Same, truncated	9.084	8.990	5.167
<b>Z = 11</b>			
Uniform	5.500	4.213	4.213
Same, truncated	5.500	4.853	4.853
Log-normal, $\sigma^* = 1$	7.012	5.781	3.736
Same, truncated	7.012	6.544	4.830
Log-normal, $\sigma^* = 0.25$	9.332	8.675	2.688
Same, truncated	9.332	9.252	5.157

threshold for transport is a simple addition of the bond thresholds along the minimal path, any rescaling of the  $\Delta V_i^{\min}$  distribution to  $\{a\Delta V_i^{\min} + b\}$ , with  $a > 0$ , similarly rescales the resulting value of  $\nabla V^{\min}$  without changing the structure of the minimal path. Therefore, for com-

parison of the  $\Delta V_i^{\min}$  distributions, we have rescaled our results so that (1) the percolation threshold for each distribution remains at 10.5 (midway between  $\Delta V_i^{\min} = 10$  and 11) and (2)  $\langle \Delta V_i^{\min} \rangle_p = 5.5$  in all cases as for the uniform distributions. This rescaled result is entitled “rescaled Bethe tree” in Fig. 9. It reveals the effect of skewness in the low end of the  $\Delta V_i^{\min}$  distribution, and in particular the effect of a tail of very low values of  $\Delta V_i^{\min}$ . Except for truncated distributions, the rescaled Bethe-tree results show a trend opposite to that of the simple percolation model: The rescaled Bethe tree  $\nabla V^{\min}$  is smaller for cases in which the simple-percolation estimate is larger. The rescaled Bethe-tree result allows comparisons on the basis of (1) the same percolation-threshold value  $\Delta V_c$  and (2) the same average value of  $\Delta V_i^{\min}$  for the portion of the distribution below  $\Delta V_c$ , i.e., the same value of  $\langle \Delta V_i^{\min} \rangle_p$ .

Consider the case of  $Z=5$  and a log-normal  $\Delta V_i^{\min}$  distribution with  $\sigma^* = 0.25$  [Fig. 8(c)]. The percolation-threshold value of  $\Delta V_i^{\min}$ ,  $\Delta V_c$ , is between 10 and 11. The average  $\Delta V_i^{\min}$  value for  $\Delta V_i^{\min}$  less than  $\Delta V_c$ ,  $\langle \Delta V_i^{\min} \rangle_p$ , is 9.084, which is the simple-percolation estimate of  $\nabla V^{\min}$  (Table III). There exists a finite fraction of bonds with  $\Delta V_i^{\min}$  as low as 1, however, well below  $\langle \Delta V_i^{\min} \rangle_p$ . The minimal path on the Bethe tree accesses these bonds more heavily than predicted by the simple percolation model, producing a lower value of  $\nabla V^{\min}$ , 8.420. Rescaling to eliminate the effects of the higher value of  $\langle \Delta V_i^{\min} \rangle_p$  for this distribution gives a value of  $\nabla V^{\min}$ , 3.157, much lower than for the other distributions. Accessing the low end of the  $\Delta V_i^{\min}$  distribution most heavily evidently requires a large fraction of bonds with  $\Delta V_i^{\min}$  just above  $\Delta V_c$ . In the truncated distribution, where all such bonds have extremely large  $\Delta V_i^{\min}$ , skewness in the tail of the  $\Delta V_i^{\min}$  distribution has little effect on the rescaled Bethe-tree result (Fig. 9): It just isn’t worth it to pass through high- $\Delta V_i^{\min}$  bonds to access clusters of bonds with low  $\Delta V_i^{\min}$ . Hence the Bethe tree  $\nabla V^{\min}$  is closer to the simple-percolation estimate.

To summarize, the minimal path does not sample the percolation-threshold fraction of small- $\Delta V_i^{\min}$  values randomly: It samples the low end of this distribution most heavily. As a result, the Bethe tree  $\nabla V^{\min}$  is lower than the simple-percolation estimate in all cases tested. The minimal path samples the low end of the  $\Delta V_i^{\min}$  distribution most heavily, however, when there are (1) a tail extending to extremely low values of  $\Delta V_i^{\min}$  and (2) a significant fraction of bonds with  $\Delta V_i^{\min}$  just above the percolation-threshold value  $\Delta V_c$ . Evidently, the path passes through an occasional bond with  $\Delta V_i^{\min} > \Delta V_c$  to access clusters of bonds with low values of  $\Delta V_i^{\min}$ .

Our limited results for the Bethe tree do not show a consistent trend with coordination number  $Z$ , except as identified by the simple percolation model [Eqs. (1) and (2)]: Because the percolation threshold is lower with larger  $Z$ ,  $\Delta V^{\min}$  depends on a smaller fraction of the overall  $\Delta V_i^{\min}$  distribution with increasing  $Z$ .

Sample results for the limiting case in which  $\Delta V_i^{\min}$  takes only values of 0 (with probability  $p$ ) and 1 are shown in Fig. 5. The distinction between the Bethe tree

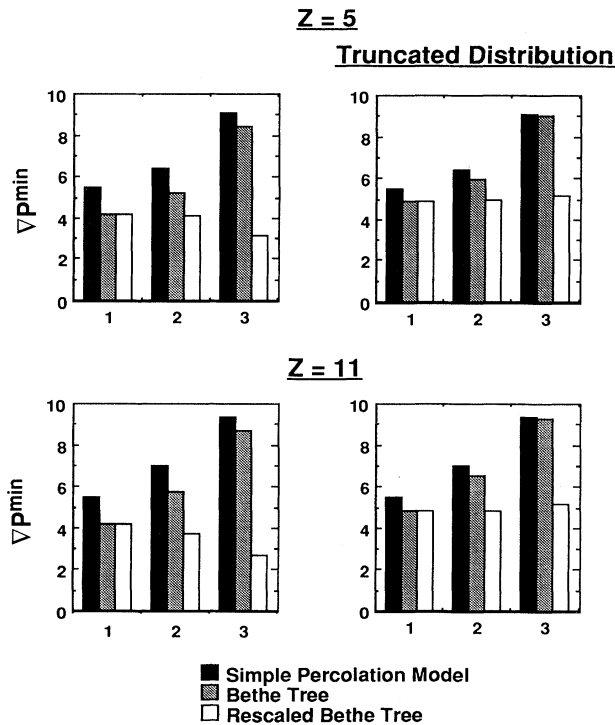


FIG. 9. Effect of bond-threshold distribution on macroscopic threshold for flow. Case 1: uniform distribution. 2: log-normal,  $\sigma^* = 1$ . 3: log-normal,  $\sigma^* = 0.25$ .

and simple percolation models is marked as  $p$  approaches  $p_c$ , even though the simple percolation model matches the asymptotic scaling exponent of the Bethe tree [Eqs. (3) and (7)]. This represents the extreme case of a skewed distribution of  $\Delta V_i^{\min}$  values, since one can form a nearly complete path for transport from bonds with  $\Delta V_i^{\min}$  values infinitely smaller than the rest of the distribution. For  $Z = 5$  and  $(p_c - p) = 0.01$ , the Bethe-tree model gives  $\nabla V^{\min} \approx 1/175$ , seven times lower than the simple percolation model. The differences increase as  $p$  approaches  $p_c$ .

None of the models examined here include the effect of "tortuosity" in the critical path for flow, in that every path leads directly across the network. The macroscopic threshold for transport  $\nabla V^{\min}$  would of course be larger for real 2D and 3D networks because at each node the critical path must choose between the lowest-threshold bond, which may or may not lead in the overall direction of the path, and the most direct path, which may or may not include the lowest-threshold bonds. In both models studied here, every alternative path leads directly across the network. It would be valuable to identify the competing effects of path length and bond-threshold distribution on the formation and structure of the minimal path in future studies.

## VI. SUMMARY

We compare two models for the onset of transport through a network with a randomly assigned threshold

for transport in each of the bonds. Neither of the models we have presented accounts for tortuosity.

We present two solutions for the minimal path in a Bethe tree: one a recursive method and one a direct method that relies on the attainment of an unchanging shape in the function  $\Delta V^{\min}(n)$ . The two methods give good agreement on the value of the potential gradient  $\nabla V^{\min}$  at which transport begins. A simple percolation model, in which the minimal path samples randomly from the percolation-threshold fraction of bonds with low microscopic thresholds, also performs remarkably well. This success may reflect in part canceling effects of two artifacts in the model: lack of tortuosity and lack of flexibility to select low-threshold bonds. The Bethe-tree estimate of  $\nabla V^{\min}$  is *much* lower than for the other models if (1) the distribution of bond thresholds  $\Delta V_i^{\min}$  has a tail of very low values and (2) there is a significant fraction of bonds with  $\Delta V_i^{\min}$  just above the value at the percolation threshold.

## ACKNOWLEDGMENTS

This work was supported in part by The Petroleum Research Fund, administered by the American Chemical Society. A. S. Sikandar helped in the statistical analysis of the Bethe-tree results. We thank Drs. M. Sahimi and P. M. Duxbury for valuable discussions.

\*Author to whom correspondence should be addressed.

†Present address: Department of Chemical Engineering, The University of Texas at Austin, Austin, Texas.

<sup>1</sup>D. Stauffer, *Introduction to Percolation Theory* (Taylor and Francis, London, 1985).

<sup>2</sup>R. M. Bradley, D. Kung, S. Doniach, and P. N. Strenski, *J. Phys. A* **20**, L911 (1987).

<sup>3</sup>S. Roux, A. Hansen, and E. Guyon, *J. Phys. (Paris)* **48**, 2125 (1987).

<sup>4</sup>S. Roux, H. Herrmann, A. Hansen, and E. Guyon, *C. R. Acad. Sci. Ser. B* **305**, 943 (1987).

<sup>5</sup>F. F. Barbosa and S. L. A. de Queiroz, *J. Phys. Condens. Matter* **1**, 2771 (1989).

<sup>6</sup>E. Meilikhov and Y. Gershanov, *Physica C* **157**, 431 (1989).

<sup>7</sup>S. Roux, A. Hansen, L. R. da Silva, L. S. Lucena, and R. B. Pandey, *J. Stat. Phys.* **65**, 183 (1991).

<sup>8</sup>M. Sahimi, *AIChE J.* (to be published).

<sup>9</sup>S. Roux and H. J. Herrmann, *Europhys. Lett.* **4**, 1227 (1987).

<sup>10</sup>R. B. Stinchcombe, P. M. Duxbury, and P. Shukla, *J. Phys. A* **19**, 3903 (1986).

<sup>11</sup>Y. C. Yortsos (unpublished).

<sup>12</sup>P. G. de Gennes, *Rev. Inst. Fr. Pét.* **47**, 249 (1992).

<sup>13</sup>P. M. Adler and H. Brenner, *Physicochem. Hydrodyn.* **5**, 287 (1984).

<sup>14</sup>P. M. Duxbury, P. D. Beale, and P. L. Leath, *Phys. Rev. Lett.* **57**, 1052 (1986).

<sup>15</sup>L. de Arcangelis, S. Redner, and A. Coniglio, *Phys. Rev. B* **34**, 4656 (1986).

<sup>16</sup>P. M. Duxbury, P. L. Leath, and P. D. Beale, *Phys. Rev. B* **36**, 367 (1987).

<sup>17</sup>B. Kahng, G. G. Batrouni, and S. Redner, *J. Phys. A* **20**, L827 (1987).

<sup>18</sup>B. Kahng, G. G. Batrouni, S. Redner, L. de Arcangelis, and H. J. Herrmann, *Phys. Rev. B* **37**, 7625 (1988).

<sup>19</sup>G. J. Hirasaki, *J. Pet. Technol.* **41**, 449 (1989).

<sup>20</sup>G. J. Hirasaki, SPE 19518 (Society of Petroleum Engineers, Richardson, TX, 1989).

<sup>21</sup>W. R. Rossen, in *Foams, Theory, Measurements, and Applications*, edited by R. K. Prud'homme and S. Khan (Marcel Dekker, New York, in press).

<sup>22</sup>R. B. Bird, W. E. Stewart, and E. N. Lightfoot, *Transport Phenomena* (Wiley, New York, 1960).

<sup>23</sup>A. H. Falls, J. J. Musters, and J. Ratulowski, *SPE Reserv. Eng.* **4**, 55 (1989).

<sup>24</sup>W. R. Rossen, *J. Colloid Interface Sci.* **136**, 1 (1990).

<sup>25</sup>W. R. Rossen, *J. Colloid Interface Sci.* **136**, 17 (1990).

<sup>26</sup>W. R. Rossen, *J. Colloid Interface Sci.* **136**, 38 (1990).

<sup>27</sup>W. R. Rossen, *J. Colloid Interface Sci.* **139**, 457 (1990).

<sup>28</sup>F. Friedmann, W. H. Chen, and P. A. Gauglitz, *SPE Reserv. Eng.* **6**, 37 (1991).

<sup>29</sup>C. J. Radke and J. V. Gillis, *Proceedings of the Annual Meeting of the Society of Petroleum Engineers, New Orleans, September, 1990* (Society of Petroleum Engineers, Richardson, TX, 1990).

<sup>30</sup>A. H. Falls, G. J. Hirasaki, T. W. Patzek, P. A. Gauglitz, D. D. Miller, and T. Ratulowski, *SPE Reserv. Eng.* **3**, 884 (1988).

<sup>31</sup>W. R. Rossen, *J. Phys. A* **21**, L533 (1988).

<sup>32</sup>W. R. Rossen and P. A. Gauglitz, *AIChE J.* **36**, 1176 (1990).

<sup>33</sup>W. R. Rossen, *J. Phys. A* **24**, 5155 (1991).

<sup>34</sup>W. R. Rossen, Z. H. Zhou, and C. K. Mamun, *Proceedings of*

- the Annual Meeting of the Society of Petroleum Engineers, Dallas, October, 1991* (Society of Petroleum Engineers, Richardson, TX, 1991).
- <sup>35</sup>S. Kirkpatrick, *Rev. Mod. Phys.* **45**, 547 (1973).
- <sup>36</sup>R. E. Collins, *Flow of Fluids Through Porous Materials* (Research and Engineering Consultants, Englewood, CO, 1990).
- <sup>37</sup>L. W. Lake, *Enhanced Oil Recovery* (Prentice-Hall, Englewood Cliffs, NJ, 1989).
- <sup>38</sup>G. R. Jerauld, H. T. Davis, and L. E. Scriven, *Proceedings of the SPE/DOE Symposium on Enhanced Oil Recovery, Tulsa, April, 1984* (Society of Petroleum Engineers, Richardson, TX, 1991).

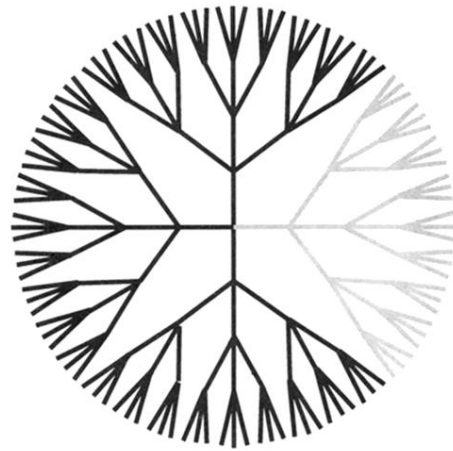


FIG. 1. Fragment of radius 4 from a Bethe tree of coordination number  $Z=4$ . One branch is highlighted.